

DISCOVERY OF A SATELLITE OF THE LARGE TRANS-NEPTUNIAN OBJECT (225088) 2007 OR₁₀

CSABA KISS,¹ GÁBOR MARTON,¹ ANIKÓ FARKAS-TAKÁCS,¹ JOHN STANSBERRY,² THOMAS MÜLLER,³ JÓZSEF VINKÓ,^{1,4} ZOLTÁN BALOG,⁵
JOSE-LUIS ORTIZ,⁶ AND ANDRÁS PÁL¹

¹*Konkoly Observatory, Research Centre for Astronomy and Earth Sciences, Hungarian Academy of Sciences, Konkoly Thege 15-17, H-1121 Budapest, Hungary*

²*Space Telescope Science Institute, 3700 San Martin Dr., Baltimore, MD 21218, USA*

³*Max-Planck-Institut für extraterrestrische Physik, Postfach 1312, Giessenbachstr., D-85741 Garching, Germany*

⁴*Department of Optics and Quantum Electronics, University of Szeged, Dóm tér 9, H-6720 Szeged, Hungary*

⁵*Max-Planck-Institut für Astronomie, Königstuhl 17, D-69117 Heidelberg, Germany*

⁶*Instituto de Astrofísica de Andalucía - CSIC, Apt 3004, E-18080 Granada, Spain*

ABSTRACT

2007 OR₁₀ is currently the third largest known dwarf planet in the Transneptunian region, with an effective radiometric diameter of ~ 1535 km. It has a slow rotation period of ~ 45 h that was suspected to be caused by tidal interactions with a satellite undetected at that time. Here we report on the discovery of a likely moon of 2007 OR₁₀, identified on archival Hubble Space Telescope WFC3/UVIS system images. Although the satellite is detected at two epochs, this does not allow an unambiguous determination of the orbit and the orbital period. A feasible $1.5\text{--}5.8\cdot 10^{21}$ kg estimate for the system mass leads to a likely 35 to 100 d orbital period. The moon is about $4^m.2$ fainter than 2007 OR₁₀ in HST images that corresponds to a diameter of 237 km assuming equal albedos with the primary. Due to the relatively small size of the moon the previous size and albedo estimates for the primary remains unchanged. With this discovery all trans-Neptunian objects larger than 1000 km are now known to harbour satellites, an important constraint for moon formation theories in the young Solar system.

Keywords: methods: observational — techniques: photometric — astrometry — minor planets, asteroids:
general — Kuiper belt objects: individual (2007OR10)

arXiv:1703.01407v1 [astro-ph.EP] 4 Mar 2017

1. INTRODUCTION

(225088) 2007 OR₁₀ (2007 OR₁₀ hereafter for short) is a large ($D \approx 1500$ km) and distant (currently at $r_{\text{helio}}=87$ AU) trans-Neptunian object (TNO). In a recent study, Pál et al. (2016) analysed light curves of 2007 OR₁₀ obtained with the K2 mission of the Kepler Space Telescope. They found that 2007 OR₁₀ rotates very slowly relative to other trans-Neptunian objects, with a most likely period of $P_{\text{rot}} = 44.81 \pm 0.37$ h. The canonical explanation of slow rotation for large bodies is tidal interaction with a fairly massive satellite. As discussed in Pál et al. (2016) the rotation period of 2007 OR₁₀ suggests that the suspected moon would be at an apparent separation of $0'.04$ – $0'.08$ assuming tidal locking and depending on their mass ratio. However, a smaller satellite at a larger separation could have slowed down the rotation of 2007 OR₁₀ to the observed value, but may not have been massive enough to force synchronous rotation.

Assuming that the primary is the only notable body in the system the integrated thermal emission indicates that 2007 OR₁₀ has a diameter of 1535^{+75}_{-225} km, making it the third largest dwarf planet, after Pluto and Eris (Pál et al. 2016). With this diameter, 2007 OR₁₀ is larger than the officially recognised dwarf planets Makemake and Haumea. If a large satellite is present, the diameter of the primary could be correspondingly smaller. To date no satellite or binarity of 2007 OR₁₀ has been reported in the literature.

Motivated by these questions, we have checked 2007 OR₁₀ observations in the Hubble Space Telescope Archive and identified a likely satellite. In this letter we describe the putative moon's characteristics as derived from these observations.

2. OBSERVATIONS AND DATA ANALYSIS

2.1. Archival Hubble Space Telescope Observations

2007 OR₁₀ was observed with the Hubble Space Telescope at two epochs, on November 6, 2009 (proposal ID: 11644, PI: M. Brown) and on September 18, 2010 (proposal ID: 12234, PI: W. Fraser). Both proposals used similar strategies, observing the target with a set of visual range and near-infrared filters of the WFC3/UVIS and IR cameras. Due to the better spatial resolution visual range observations are preferred in identifying unknown satellites, and we used the WFC3/UVIS observations to look for potential moons of 2007 OR₁₀ in these series of measurements.

At the first epoch (November 6, 2009, 17:08:36 start time) 2007 OR₁₀ was observed with the WFC3/UVIS camera system using the 512-pixel sub-array mode with the UVIS1-C512A-SUB aperture, in a series of four measurements with the F606W-F814W-F606W-F814W filters. Each measurement lasted for 129 s. A similar strategy was followed at the second epoch (September 18, 2010, 15:54:12 start time), now taking four measurements with the UVIS2-C512C-SUB

aperture and using the F606W-F775W-F606W-F775W filter combination. The F606W measurements lasted for 128 s, while the length of the F775W measurements were 114 s (see also Table 1).

There is a faint source in the vicinity of 2007 OR₁₀ that appears in both epochs and in all images, and at the same location with respect to 2007 OR₁₀ at each epoch (see Table 1 and Fig. 1).

We used the drizzle images and routines built on the DAOPHOT-based APER function in IDL¹ to obtain aperture photometry and astrometry of the photocenters of both 2007 OR₁₀ and the suspected satellite. On the November 6, 2009 images aperture photometry could be performed for both targets separately, in both bands (F606W and F814W). In the case of the September 18, 2010 images, however, the satellite was too close to 2007 OR₁₀ and reliable photometry of the moon could only be performed after the subtraction of 2007 OR₁₀'s point spread function (PSF). This was modeled using the TinyTim (Krist et al. 2010) software, using specific setups of date, camera system, target's pixel position, focal length, and spectral energy distribution of the target (black body of 5800 K). The TinyTim-created drizzle model images were adequate to subtract the contribution of 2007 OR₁₀ from the original drizzle images. The best-fit parameters of the model PSF were determined using Levenberg-Marquardt nonlinear least-square fitting. The extracted relative positions of the satellite are listed in Table 1.

At the first observational epoch, 2007 OR₁₀ moved with an average apparent velocity of $v_{\lambda} = -0.33'' \text{ h}^{-1}$ and $v_{\beta} = -0.47'' \text{ h}^{-1}$ in Ecliptic longitude and latitude. The total motion observed in the sequence of exposures was $0'.10$ (2.5 pixels). At the second epoch, the apparent velocities were $v_{\lambda} = -1.86'' \text{ h}^{-1}$ and $v_{\beta} = 0.01'' \text{ h}^{-1}$, and the total observed motion was $\sim 0'.33$ (8 pixels). Within each epoch, the position of the secondary source relative to 2007 OR₁₀ was constant to within the measurement errors of our astrometry (see Fig. 1). Since those astrometric errors ($\sim 0'.04$) are much smaller than the observed motion of 2007 OR₁₀, we confirm that the secondary source was comoving at both epochs.

We also determined the brightness difference between 2007 OR₁₀ and its moon for each measurement (see Table 1). As in the case of relative astrometry, proper photometry was only possible after subtracting the PSF of the primary in the second epoch images.

The uncertainties in the relative brightness determination reflect the low signal-to-noise ratio of the satellite detection, especially at the first epoch, when we detected it at the 3–4 σ significance level. There is a notable change in the brightness (~ 0.3) of the satellite relative to 2007 OR₁₀ between

¹ Interactive Data Language, Harris Geospatial Solutions

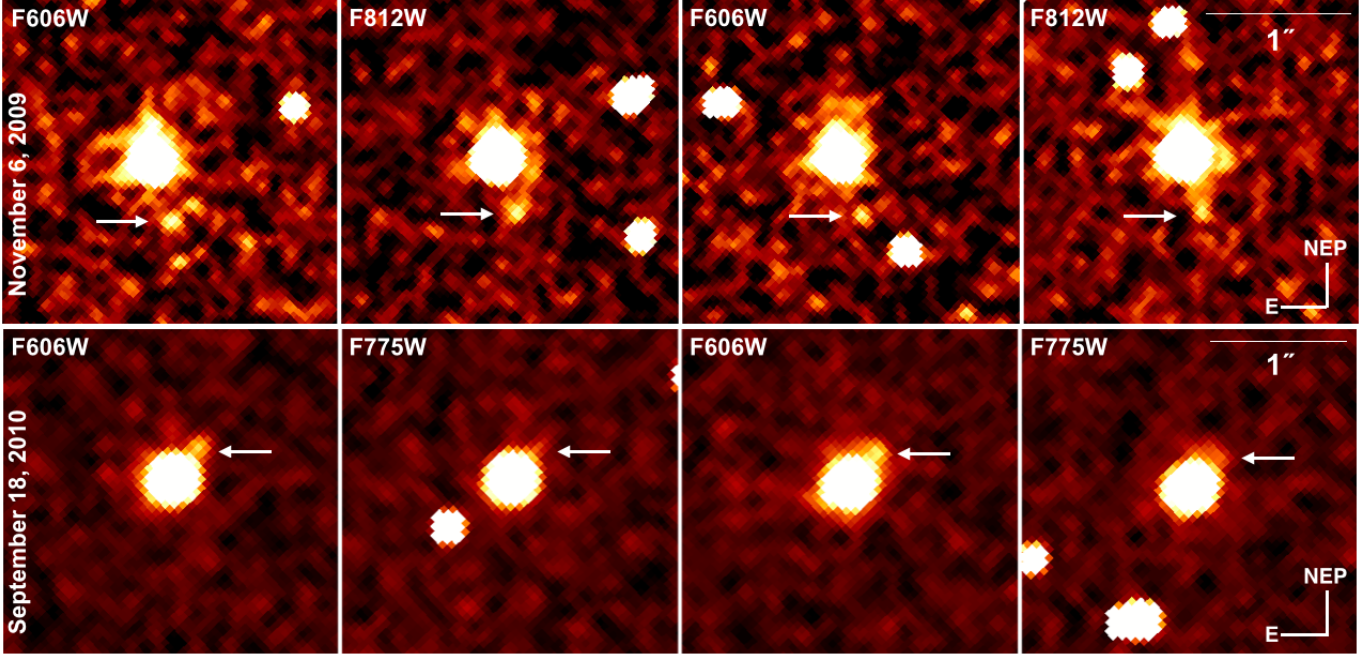


Figure 1. Hubble Space Telescope WFC3/UVIS images of 2007 OR₁₀. Upper row: November 6, 2009 measurements, F606W-F812W-F606W-F812W filter series; bottom row: September 2010 images, F606W-F775W-F606W-F775W filter series. The suspected satellite can be most readily identified on the F606W images and is marked by a white arrow on each image (North is up and East is left, in Ecliptic coordinates).

Table 1. Summary table of the derived satellite characteristics as observed on the dates (start times) and with the filters given below. The table also lists the integration times (t_{int}), the brightness difference with respect to 2007 OR₁₀ (Δm), the offset in Ecliptic coordinates relative to 2007 OR₁₀ ($\Delta\lambda, \Delta\beta$), the heliocentric (r_h) and geocentric distances (Δ) and the phase angle (α) at the time of the observations.

Epoch (JD)	Filter	t_{int} (s)	Δm (mag)	$\Delta\lambda$ ($''$)	$\Delta\beta$ ($''$)	r_h (AU)	Δ (AU)	α (deg)
2455142.2136	F606W	128	4.25 ± 0.28	-0.166 ± 0.025	-0.436 ± 0.025	85.960	85.683	0.63
2455142.2159	F814W	128	4.30 ± 0.30	-0.164 ± 0.025	-0.429 ± 0.025			
2455142.2188	F606W	128	4.61 ± 0.29	-0.162 ± 0.025	-0.423 ± 0.025			
2455142.2211	F814W	128	4.43 ± 0.38	-0.170 ± 0.040	-0.445 ± 0.040			
2455458.1619	F606W	129	4.13 ± 0.18	-0.154 ± 0.025	0.183 ± 0.025	86.175	85.263	0.27
2455458.1642	F775W	114	4.64 ± 0.30	-0.189 ± 0.040	0.188 ± 0.040			
2455458.1669	F606W	129	4.17 ± 0.19	-0.158 ± 0.025	0.182 ± 0.025			
2455458.1692	F775W	114	4.31 ± 0.23	-0.147 ± 0.040	0.199 ± 0.040			

the two epochs. As the light curve of 2007 OR₁₀ is shallow (Pál et al. 2016), only a maximum of $\sim 0^m.09$ difference can be attributed to the rotation of the primary. However, shape and/or albedo variegations on the surface of the satellite can easily account for the remaining flux difference. The mean brightness differences are found to be $\Delta m(\text{F606W}) = 4^m.23 \pm 0^m.24$, $\Delta m(\text{F775W}) = 4^m.43 \pm 0^m.30$ and $\Delta m(\text{F814W}) = 4^m.35 \pm 0^m.25$. As these are nearly equal in all bands, 2007 OR₁₀ and its satellite have very similar colors

from the V to the I bands, roughly covered by the three HST/WFC3 filters used. We find it very unlikely that two independent, co-moving sources with similar brightness and both having the same color as 2007 OR₁₀ would be found in the vicinity of 2007 OR₁₀ at two epochs. Therefore we hypothesize that the two sources we found at the two epochs are two appearances of the same satellite.

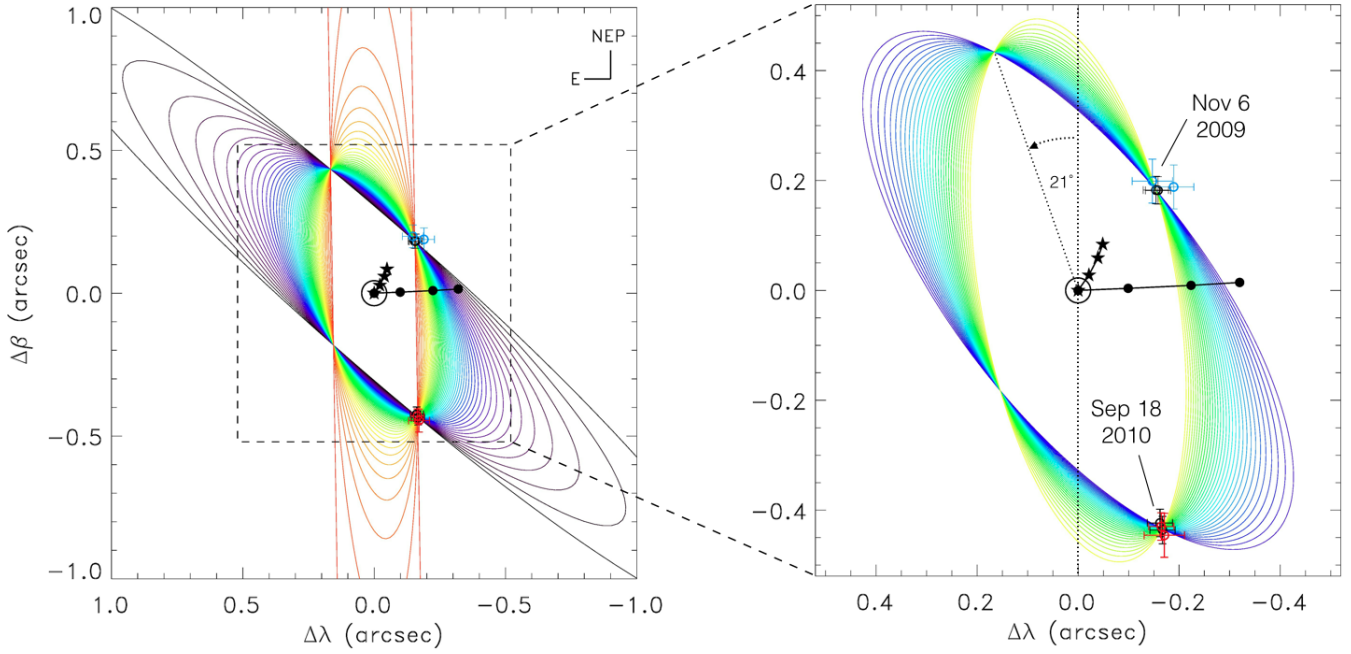


Figure 2. Relative positions of two sources, one at each epoch, identified as the putative satellite, in ecliptic coordinates, with respect to 2007 OR₁₀. The sources are marked by open circles with error bars, 2007 OR₁₀ is the large open circle in the center. The colours of the satellite positions correspond to different filters: F606 - black; F755W - blue; F812W - red. The sources co-move with 2007 OR₁₀ in the two series of images, i.e. their positions are the same in this figure, within the uncertainties. Curves connecting black dots and stars starting from the center indicate the movement of 2007 OR₁₀ with respect to the background between the exposures during the November 6, 2009 (stars) and September 18, 2010 (filled circles). We plot the ellipses best fit to the observed positions of the source, assuming that 2007 OR₁₀ is in the centre (projection of circular orbits). The right panel is a magnified view of the innermost $\sim 1'' \times 1''$ region, showing only those ellipses that fit into the window

With these colours both 2007 OR₁₀ and the satellite are among the reddest objects known in the trans-Neptunian region.

In general, red TNOs are seen to have higher albedos than gray objects (see [Lacerda et al. 2014](#)). Since both 2007 OR₁₀ and the satellite are extremely red, our data suggest that they are likely to have similar albedos, and that the albedo of 2007 OR₁₀ ($p_V = 0.089$) probably applies to the satellite as well.

For the 2007 OR₁₀ system we adopt the absolute magnitudes and colours found in [Boehnhardt et al. \(2014\)](#), i.e. $H_V = 2^m34$, $H_R = 1^m49$, $B-V = 1^m38$, $V-R = 0^m86$, $R-I = 0^m79$. Consideration of the contribution of the satellite to the total brightness of the system increases the absolute brightness magnitude of 2007 OR₁₀ by $\sim 0^m03$, while the colors are nearly unchanged. This results in $H_V = 6^m57 \sim 0^m26$ for the satellite. We use this value in the size and thermal emission calculations below.

2.2. Possible orbits of the satellite

The two set of observations allowed us to set some constraints on the orbit of the satellite around 2007 OR₁₀. We assume that the orbit of the satellite is circular as circularisation times are typically significantly shorter than the age

of these systems ([Noll et al. 2008](#)). Then, the apparent ellipse of the orbit is a projection of the circular orbit, with 2007 OR₁₀ in the center in a co-moving frame. The two orbital positions defined by the two set of observations do not determine the orbit unambiguously, but allow a family of ellipses to be fitted, as presented in Fig. 2. In our case the possible position angles of the ellipses range from 1° to 51° (from North to East in Ecliptic coordinates). The semi-major and semi-minor axes of the smallest ellipse are $0'.46$ and $0'.22$ (29300 and 13600 km) with 21° position angle. For smaller and larger values within the 1° to 51° range the semi-major axes increase quickly and get infinitely large at the limiting position angles.

A reliable estimate for the mass of 2007 OR₁₀ can be obtained using the size limits of the thermophysical model calculations ([Pál et al. 2016](#)), $D_{\text{eff}} = 1310\text{--}1610$ km. As 2007 OR₁₀ is a fairly large object, internal porosity is likely negligible and a lower limit for the density can be set to 1.2 g cm^{-3} , a typical value for medium size TNOs ([Brown 2013](#); [Barr & Schwamb 2016](#); [Kovalenko et al. 2017](#)). For an upper limit we use the densities of the largest dwarf planets Pluto and Eris, and adopt 2.5 g cm^{-3} . With these assumptions the mass of 2007 OR₁₀ would be $1.5\text{--}5.8 \cdot 10^{21}$ kg. Then,

with the smallest possible semi-major axis the orbital periods would be $18^{\text{d}}.5\text{--}36^{\text{d}}.4$, depending on the system mass assumed.

The two observed positions also define the orbital phases for a specific orbit (ellipse), and the phase difference can be used to find those orbital periods that are compatible with the observed positions, considering the time spent between the two set of observations ($315^{\text{d}}.95$). The semi-major axis and the orbital period also defines the system mass according to Kepler’s third law. We applied this scheme to all ellipses fitted to the two satellite positions, determined the compatible orbital periods and calculated the related systems mass values. The results are presented in Fig. 3. The shortest orbital periods compatible with the phase differences for any of the fitted ellipses are $19^{\text{d}}.05$ for prograde (black dots) and $19^{\text{d}}.23$ for retrograde (red dots) sense of revolution. Shorter orbital periods would require a mass too high for our upper limits (upper-left corner in Fig. 3). Although only some well-defined orbital periods are allowed there, there are several of these possible orbital period groups in the 20 to 100 day range. This means that neither the orbital period nor the system mass can be constrained further by the two existing HST observations. Although they cannot be fully excluded, orbital periods longer than ~ 100 d become increasingly unlikely as the satellite would spend most of the time at large apparent distances. We have found three groups of possible periods at ~ 126 , ~ 210 and ~ 630 d, but no additional orbital periods were identified for > 1000 d.

The expected orbital period of a satellite can be estimated using the formalism in Murray & Dermott (1999), assuming tidal dissipation and requiring that the current semi-major axis is significantly different from the initial one. In this case the orbital period is $P \propto k^{3/13} Q^{-3/13} q^{-3/13} m_p^{-5/13}$, where k is the tidal Love number, Q is the quality factor of the primary, q is the ratio of the primary to the satellite mass and m_p is the mass of the primary. With some reasonable assumptions for these parameters (see also Brown & Schaller 2007; Brown et al. 2007), and assuming an evolution of 4.5 Gyr we can estimate the possible orbital periods. In the equal albedo and equal density case the mass ratio is $q \approx 350$, and the high and low mass limits for the primary gives orbital periods between 45 and 76 days. Orbital periods around 35 days require a significant ($> 2.5\times$) internal density difference between the primary and the moon. This is, however, reasonable concerning the known higher densities of the largest and the mid-sized trans-Neptunian objects (see e.g. Brown 2013; Kovalenko et al. 2017). In the case of a low albedo moon ($p_V \approx 5\%$) and a low mass primary the orbital period would be $P \approx 100$ d. These calculations show that the preferred orbital periods are in the range of 35 to 100 d, and that the orbits with the smallest semi-major axes and shortest periods ($P \approx 20$ d) may not be the most likely ones.

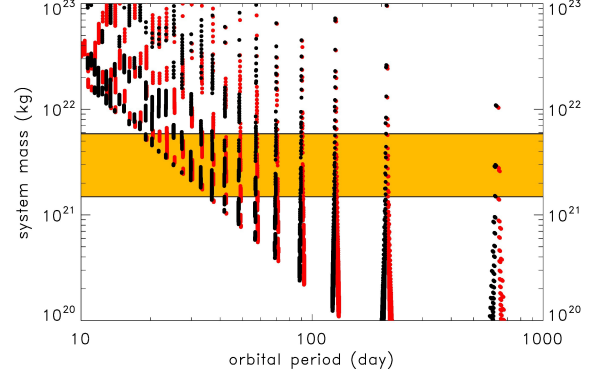


Figure 3. Possible system mass values based on the fitted orbits and the observed orbital phase differences. The orange region shows the mass range based on an assumed range of density and size of 2007 OR₁₀. Possible prograde and retrograde solutions are marked by black and red dots.

3. THERMAL EMISSION OF THE SYSTEM

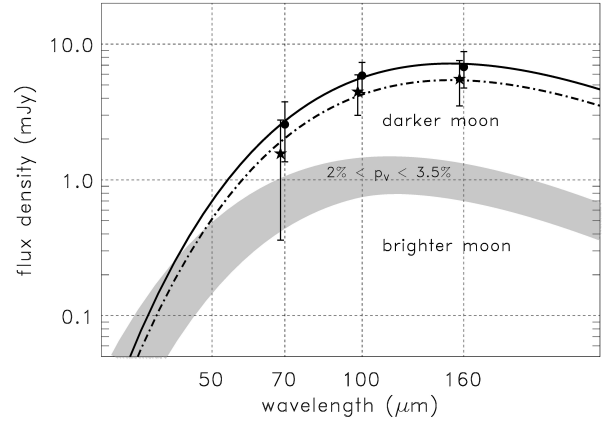


Figure 4. Thermal emission components in the 2007 OR₁₀ system. The black dots with error bars represent the measured Herschel/PACS fluxes. The thick black curve is the best-fit NEATM model with $D = 1535$ km and $\eta = 1.8$ for the primary (Pál et al. 2016). The gray area represent NEATM thermal emission models of the putative satellite assuming geometric albedos in the range of 2% to 3.5% (size of 350 km), with very low ($\eta < 0.8$) beaming parameter values. Stars with error bars and the related dash-dotted curve best-fit NEATM model represent the corrected thermal emission of 2007 OR₁₀ assuming an extremely dark moon (data points are slightly shifted in wavelength for clarity, see the text for details).

In the case of Makemake, a dwarf planet of similar size, the satellite may have a significant contribution to the thermal emission of the system due to the possibly large albedo difference (Lim et al. 2010; Parker et al. 2016). In the case of 2007 OR₁₀, however, the primary is rather dark: $p_V = 0.089^{+0.031}_{-0.009}$ (Pál et al. 2016). We calculated the possible contribution of the satellite to the thermal emission using the

Near-Earth Asteroid Thermal Model model ((NEATM [Harris 1998](#))) assuming geometric albedos in the range of 2% to 9% for the satellite. We used the absolute magnitude of $H_V = 6^m57 \pm 0^m26$ determined above and applied the formula by [Brucker et al. \(2009\)](#) to obtain the phase integral and the Bond albedo. The upper limit of $p_V = 9\%$ we considered is the geometric albedo of the primary: in the case of higher albedos the contribution of the satellite would be negligible due to the large primary to satellite area ratio (>40). We allowed the beaming parameter η to vary in the range of 0.6–2.5 (see e.g. [Lellouch et al. 2013](#)). The far-infrared flux densities of the system, as observed with Herschel/PACS at 70, 100 and 160 μm , are taken from [Pál et al. \(2016\)](#).

As presented in Fig. 4, only extremely dark ($p_V = 2\text{--}3.5\%$) and rough ($\eta < 0.8$) surfaces provide a noticeable contribution to the total thermal emission. While such surfaces exist among Solar system bodies (e.g. [Pál et al. 2015](#)) the geometric albedos in the trans-Neptunian region are typically higher than this. The dark-neutral population of objects ([Lacerda et al. 2014](#)) have typical geometric albedos of $p_V \approx 5\%$, but practically no objects show $p_V < 4\%$. In the scattered disk which is the dynamical class of 2007 OR₁₀ the typical geometric albedos are between 4% and 9%.

We have recalculated the best fit NEATM models for 2007 OR₁₀ itself by correcting the measured Herschel/PACS flux for the contribution of a satellite with extremely low albedo and beaming parameter.

In this case the satellite would have $p_V = 0.02$, $\eta = 0.6$, and a corresponding diameter of ~ 450 km, resulting in flux densities of 0.99, 1.37 and 1.24 mJy in the Herschel/PACS 70, 100 and 160 μm bands. After correcting for this contribution, the best fit models for 2007 OR₁₀ itself prefer high beaming parameter values of $\eta \approx 2.5$, with $D_{\text{eff}} \approx \sim 1500$ km. However, these high η values are very unlikely given the slow rotation of 2007 OR₁₀. Therefore we also calculated the best fit size of the primary using a fixed beaming parameter value of $\eta = 1.8$, too, the best fit η obtained in [Pál et al. \(2016\)](#) (dashed line in Fig. 4). This provides $D_{\text{eff}} = 1360$ km and a corresponding geometric albedo of $p_V = 0.11$. This size is still larger than the previous estimate for 2007 OR₁₀ by [Santos-Sanz et al. \(2012\)](#) and also that of Haumea ([Fornasier et al. 2013](#), $1240^{+68.7}_{-58}$ km), but smaller than that of Makemake ([Ortiz et al. 2012](#), 1430–1502 km). We emphasise again that this is an extreme situation any realistic surface assumed for the satellite ($p_V \geq 0.04$) leaves the [Pál et al. \(2016\)](#) size estimate ($D \approx 1535$ km) unchanged.

4. THE IMPORTANCE OF THE SATELLITE OF 2007 OR₁₀

Multiple systems are very useful tools for unraveling the main physical properties of trans-Neptunian objects (see e.g. [Noll et al. 2008](#)), When diameter measurements are

available, these are the only cases when a reliable estimate of the average density can be obtained. Densities provide information on the internal structure and formation processes ([Brown 2013](#); [Vilenius et al. 2014](#); [Grundy et al. 2015](#); [Barr & Schwamb 2016](#)).

In a recent paper [Parker et al. \(2016\)](#) reported on a possible discovery of a moon around the dwarf planet Makemake. However, the satellite was identified at a single epoch only. Existence of a moon orbiting 2007 OR₁₀ would mean that all known Kuiper belt objects larger than ~ 1000 km host satellites, including the four recognized outer dwarf planets: Pluto, Eris, Makemake, Haumea, plus Orcus and Quaoar (the sample discussed in [Barr & Schwamb \(2016\)](#)), and now 2007 OR₁₀.

While the densities in the additional cases (Makemake and 2007 OR₁₀) are not yet known, we can estimate the mass ratios, q , assuming some realistic albedos and near-equal densities. For Makemake the 7^m0 magnitude difference ([Parker et al. 2016](#)) results in $q = 2 \cdot 10^{-5} - 5 \cdot 10^{-4}$, assuming equal or darker albedos for the satellite than that of the primary. For 2007 OR₁₀ equal albedos give $q = 0.004$, low albedos for the satellite result in $q \approx 0.01$. With these mass ratios all large bodies in our list have $q < 0.1$ and most systems have $q \approx 0.01$.

Binaries smaller than 1000 km tend to have nearly equal brightness values, and therefore likely have $q > 0.1$ (see e.g. [Noll et al. 2008](#), for a review). Near-equal binaries are natural outcome of dynamical capture models (e.g. [Astakhov et al. 2005](#)) while collisional simulations ([Durda et al. 2004](#); [Canup 2005](#)) can explain the low mass ratios of the satellites of the largest bodies. The fact that now *all* Kuiper belt objects with diameters larger than ~ 1000 km have satellites underlines the importance of such collisions and may give constraints on the physical conditions in the still dynamically cold disk in the young Solar system.

With the determination of 2007 OR₁₀'s satellite's orbit by future observations we will also be able to put constraints on the level of possible tidal dissipation and estimate whether the satellite alone could have slowed down the rotation of 2007 OR₁₀ to the observed ~ 45 h value. The bulk density of the 2007 OR₁₀ system would also be of significant interest, especially in comparison with that of Makemake, an object of very similar size ($D \approx 1430$ km), but with much higher albedo (0.4, vs. 0.09 for 2007 OR₁₀) and covered in volatile CH₄ ice ([Brown et al. 2015](#); [Lorenzi et al. 2015](#)).

Data presented in this paper were obtained from the Mikulski Archive for Space Telescopes (MAST). STScI is operated by the Association of Universities for Research in Astronomy, Inc., under NASA contract NAS5-26555. Support for MAST for non-HST data is provided by the NASA Office of Space Science via grant NNX09AF08G and by other grants and contracts. The research leading to these results has re-

ceived funding from the European Union’s Horizon 2020 Research and Innovation Programme, under Grant Agreement no 687378; from the GINOP-2.3.2-15-2016-00003 grant of the National Research, Development and Innovation Office (Hungary); and from the LP2012-31 grant of the Hungarian Academy of Sciences. Funding from Spanish grant AYA-

2014-56637-C2-1-P is acknowledged, as is the Proyecto de Excelencia de la Junta de Andalucía, J. A. 2012-FQM1776.

Facilities: HST(STIS)

REFERENCES

- Astakhov, S.A., Lee, E.A., Farrelly, D., 2005, MNRAS, 360, 401
- Barr, A. C., Schwamb, M. E., 2016, MNRAS, 460, 1542
- Canup, R.M., 2005, Science, 307, 546
- Boehnhardt, H., Schulz, D., Protopapa, S., Götz, C., 2014, EM&P, 114, 35
- Brown, M.E., van Dam, M.A., Bouchez, A.H., 2006, ApJ, 639, L43
- Brown, M.E., Schaller, L., 2007, Science, 316, 1585
- Brown, M.E., Bouchez, A.H., Rabinowitz, D., et al., 2007, ApJ, 623, L45
- Brown, M.E., 2013, ApJ, 778L, 34B
- Brown, M.E., Schaller, E.L., Blake, G.A., 2015, AJ, 149, 105
- Brucker, M.J., Grundy, W.M., Stansberry, J.A., et al., 2009, Icarus, 201, 284
- Burkhart, L.D., Ragozzine, D., Brown, M.E., 2016, AJ, 151, 162
- Dressel, L., 2016. “Wide Field Camera 3 Instrument Handbook, Version 8.0” (Baltimore: STScI)
- Durda, D.D., Bottke, W.F.; Enke, B.L., et al., 2004, Icarus, 170, 243
- Fornasier, S., Lellouch, E., Müller, T.G., et al., 2013, A&A, 555, A15
- Grundy, W. M., Porter, S. B., Benecchi, S. D. et al., 2015, Icarus, 257, 130
- Harris, A.W., 1998, Icarus, 131, 291
- Kovalenko, I.D., Doressoundiram, A., Lellouch, E., et al., 2017, A&A, submitted
- Krist, J., Hook, R., Stoehr, F., 2010ascl.soft10057K
- Lacerda, P., Fornasier, S., Lellouch, E., et al., 2014, ApJ, 793, L2
- Lellouch, E., Santos-Sanz, P., Lacerda, P., et al., 2013, A&A, 557, A60
- Lim, T., Stansberry, J., Müller, T.G., et al., 2010, A&A, 518, L148
- Lorenzi, V., Pinilla-Alonso, N., Licandro, J., 2015, A&A, 577, A86
- Murray, C.D. & Dermott, S.F., 1999, Solar System Dynamics, Cambridge University Press, New York
- Noll, K. S., Grundy, W. M., Chiang, E. I., Margot, J.-L., Kern, S. D., 2008, “Binaries in the Kuiper Belt”, in: The Solar System Beyond Neptune, University of Arizona Press
- Ortiz, J.-L., Sicardy, B., Braga-Ribas, F., et al., 2012, Nature, 491, 566
- Pál, A., Kiss, Cs., Horner, J., 2015, A&A, 583, A93
- Pál, A., Kiss, Cs., Müller, T.G., et al., 2016, AJ, 151, 117
- Parker, A.H., Buie, M.W., Grundy, W.M., Noll, K.S., 2016, ApJ, 825, L9
- Santos-Sanz, P., Lellouch, E., Fornasier, S., et al., 2012, A&A, 541, A92
- Vilenius, E., Kiss, C., Müller, T., Mommert, M. et al., 2014, A&A, 564, A35